Available online at www.sciencedirect.com
ScienceDirect
Journal of Photochemistry and Photobiology A: Chemistry 189 (2007) 398–404
Journal of Photochemistry and Photobiology A:Chemistry
www.elsevier.com/locate/jphotochem

Synthesis, optical and initiating properties of new two-photon polymerization initiators: 2,7-Bis(styryl)anthraquinone derivatives

Jin-Feng Xing [a,b], Wei-Qiang Chen [a], Xian-Zi Dong [a], Takuo Tanaka [c], Xiang-Yun Fang [d], Xuan-Ming Duan [a,*], Satoshi Kawata [c]

[a] *Laboratory of Organic NanoPhotonics, Technical Institute of Physics and Chemistry, Chinese Academy of Sciences, No. 2, Beiyitiao, Zhongguancun, Haidian District, Beijing 100080, China*
[b] *Graduate School of Chinese Academy of Sciences, Chinese Academy of Sciences, No. 2, Beiyitiao, Zhongguancun, Haidian District, Beijing 100080, China*
[c] *NanoPhotonics Laboratory, The Institute of Physical and Chemical Research (RIKEN), 2-1 Hirosawa, Wako, Saitama 351-0198, Japan*
[d] *Laboratory of Ultra-Fast Laser, Technical Institute of Physics and Chemistry, Chinese Academy of Sciences, No. 2, Beiyitiao, Zhongguancun, Haidian District, Beijing 100080, China*

Received 28 July 2006; received in revised form 27 February 2007; accepted 6 March 2007
Available online 12 March 2007

Abstract

C_{2v} symmetrical anthraquinone derivatives, 2,7-bis(2-(4-dimethylamino-phenyl)-vinyl)anthraquinone (**1**) and 2,7-bis(2-(4-methoxy-phenyl)-vinyl)anthraquinone (**2**) were synthesized by Wittig reaction. Their one-photon absorption and fluorescence, as well as two-photon absorption properties were investigated. These compounds showed strong intramolecular charge transfer bands as well as low fluorescence quantum yield. **1** showed a larger two-photon absorption cross-section of 1635 GM than that of 995 GM for **2** at the wavelength of 800 nm. Furthermore, the initiating properties of **1** and **2** were studied by two-photon induced polymerization. The resin with **1** as photoinitiator ($\boldsymbol{R_1}$) possessed higher sensitivity with a threshold energy 3.67 mW at the concentration of 0.02 wt% compared to that of 8.03 mW for **2**. The resolution of polymer line, fabricated with $\boldsymbol{R_1}$ at the threshold with the linear scan speed of 50 μm/s, is 105 nm. This investigation on the relationship of resolution and sensitivity indicated higher sensitivity benefit to the improvement of microfabrication resolution.

Keywords: Two-photon absorption; Anthraquinone derivatives; Two-photon polymerization

1. Introduction

Two-photon absorption (TPA) is a third-order nonlinear optical process and the region of TPA can be confined in a tiny volume around the focal point. Any subsequent process of TPA, such as two-photon induced fluorescence or two-photon induced polymerization (TPIP), is also localized to this small volume [1,2]. This characteristic of two-photon process has made TPIP becoming an effective tool for three dimensional lithographic microfabrication (3DLM). This new application has attracted great attention for the following reasons: (1) it can create any kind of 3D structures based on computer generated 3D models; (2) the fabrication procedure is simple and fast; (3) the spatial resolution of 3D structures can be as small as 100–200 nm; (4) the fabricated structures can be integrated into complicated devices [3,4]. Most work in this field has involved patterning structures in commercial photoresists in which the conventional ultraviolet (UV) active initiators are usually used. In general, these conventional initiators have low two-photon sensitivity because of their low TPA cross-section (δ_{TPA}). Thus, high excitation power and long exposure time are necessary to cure the resin, which often result in damage to the polymeric structure. For TPIP become a commonly applied technique, photoinitiators with high-sensitivity are desired to make the process more reliable and allow structures to be patterned rapidly [5].

To overcome the disadvantage of low δ_{TPA} of the conventional initiators, great efforts were made to improve δ_{TPA} of molecules. Several strategies have been proposed for design of molecules

* Corresponding author. Tel.: +86 10 8254 3596; fax: +86 10 8254 3597.
E-mail address: xmduan@mail.ipc.ac.cn (X.-M. Duan).

1010-6030/$ – see front matter © 2007 Elsevier B.V. All rights reserved.
doi:10.1016/j.jphotochem.2007.03.002

with large δ_{TPA} [6–11]. Plenty of TPIP initiators with large δ_{TPA} were reported and showed much higher sensitivity than conventional UV-active initiators. However, most of reported initiators possess high fluorescence quantum yields [12–16]. It means that the probability of radical generation should be lowered because the relaxation of two-photon induced excited state occurs more via irradiation process than via non-irradiation process, such as radical generation. Thus, for a TPIP initiator, it is necessary that the molecules not only have large δ_{TPA}, but also possess high capability to efficiently produce reactive intermediate radicals or cations, just like traditional UV initiators [3]. From this viewpoint, the molecules with large δ_{TPA} and lower fluorescence quantum yield, which can be expected to improve two-photon absorption efficiency and suppress irradiative relaxation of two-photon induced excited state, will be satisfied for TPIP.

Our efforts are made to design new TPIP initiator on the basis of conventional UV initiators. Anthraquinone derivatives have been extensively used as initiators for one-photon polymerization due to their unique π-conjugated system [17–20]. The quinone at the 9- or 10-position of anthraquinone can act as an excellent acceptor, and the 2-, 7-positions of anthraquinone can be easily modified to form a D-π-A-π-D type molecule by introducing electron donor. Here, we select strong electron-donating groups, dimethylamino and methoxy moiety, as donors, and use styryl to prolong π conjugated system. This kind of molecule may possess large δ_{TPA} due to the potential intramolecular charge transfer according to the previous report [11]. Besides large δ_{TPA}, these C_{2v} symmetrical molecules often show lower fluorescence quantum yield than those of the linear type [21]. Compounds with low fluorescence quantum yield are preferred for TPIP initiators because low fluorescence quantum yield should guarantee high triplet quantum yield [22–24], which usually leads initiators reacting with monomer to produce radicals or ions for initiating polymerization. In the context, we synthesized 2,7-bis(styryl)anthraquinone derivatives (**1** and **2** shown in Scheme 1) with C_{2v} symmetry, and investigated their one photon and two-photon absorption properties, as well as the TPIP initiating properties of these compounds.

2. Experiment

2.1. Materials

N-Bromosuccinimide (NBS), benzoyl peroxide (BPO), triphenylphosphine (PPh_3), methacrylic acid (MAA) and all solvent were supplied from Beijing Chemical Reagent Company. Multifunctional acrylic oligomers, dipentaerythritol hexaacrylate (DEP-6A, trade name: Light Acrylate DEP-6A), was obtained from Kyoeisha Chemical Co., Ltd., Japan. 2,7-Dimethylanthraquinone (**A**) was prepared from 2-methyl phthalic anhydride by two steps [25]. Solvents were dried over calcium hydride and freshly distilled before use. All reactions were carried out under nitrogen atmosphere.

2.2. Instruments and measurement

^{1}H NMR spectra were recorded on a Varian Jemini-300 spectrometer using CD_3OD as solvent and all shifts are referenced to TMS. The fine splitting of phenyl ring patterns is ignored and the signals are reported as simple doublets, with *J* values referring to the two most intense peaks. Infrared spectroscopic measurements were performed in the range 4000–400 cm^{-1} at a resolution of 1.0 cm^{-1} using a Brucher Tensor 27 FTIR Spectrometer. High-resolution mass spectra (HRMS) were measured on Micromass ZAB-HS. The UV–vis absorption and fluorescence spectra were recorded on a UV-2550 Shimadzu UV–vis spectrophotometer and a Hitachi F-4500 fluorescence spectrophotometer, respectively. The fluorescence quantum yields of **1** and **2** were measured in DMF solution at the concentration of 1×10^{-6} M with reference to Coumarin 307 in acetonitrile ($\Phi = 0.58$) [26].

Two-photon induced excited fluorescence (TPEF) spectra were recorded on SD2000 spectrometer (Ocean Optics), excited by mode-locked Ti-Sapphire femtosecond laser (Tsunami, Spectra-Physics) which wavelength, pulse width and repetition rate were 800 nm, 80 fs and 82 MHz, respectively. The δ_{TPA} of **1** and **2** were determined by using a non-linear transmission measurement technique following the experimental protocol described in detail by He and Xu [27]. The input light intensity varies from 0.2 to 1.3 GW/cm^2. The solutions of **1** and **2**, at the concentration of 2.9×10^{-4} M in DMF, were used for δ_{TPA} measurement with solvent DMF as reference. Under the applied intensity levels, neither backward stimulated scattering nor forward continuum generation was observed from the solution cell or the solvent cell.

2.3. Synthesis and characterizations

The synthetic route of **1** and **2** are outlined in Scheme 1.

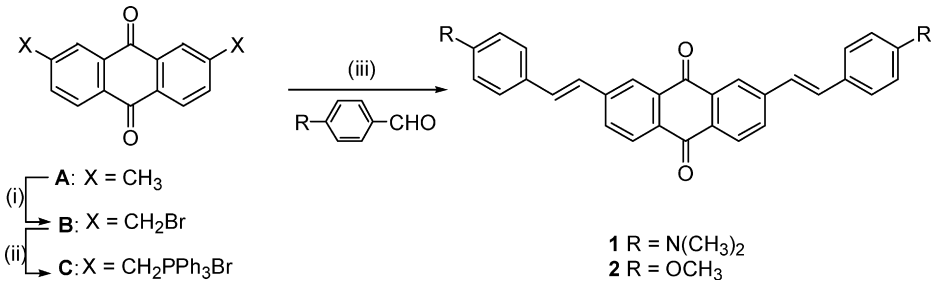

Scheme 1. The synthetic route of 1 and 2: (i) NBS, BPO, CCl_4, reflux, 24 h; (ii) PPh_3, DMF, 100 °C, 12 h; (iii) NaH, DMF, 20 h, 100 °C.

2.3.1. 2,7-Dibromomethyl-anthraquinone(B)

2,7-Dimethyl-anthraquinone (5.834 g, 24.6 mmol) and *N*-bromosuccinimide (11.413 g, 64.1 mmol) were added to a three-neck flask containing CCl_4 (400 mL). After the suspension was heated to 70 °C, benzoyl peroxide (0.760 g, 3.3 mmol) was added. The reaction suspension was heated to reflux for 24 h. After the mixture was cooled to room temperature, the precipitate was filtered, washed with water (200 mL × 3), and dried under vacuum. Recrystallization from a toluene solution gave a light yellow powder (5.838 g, 60% yield). m.p. 271–273 °C. ^{1}H NMR 300 MHz ($CDCl_3$,) δ (ppm) 8.33 (s, 2H), 8.30 (d, J = 8.1 Hz, 2H), 7.83 (d, J = 8.1 Hz, 2H), 4.60 (s, 4H).

2.3.2. 2,7-Bis-[(triphenylphosphonium bromide)]-methyl)-anthraquinone (C)

2,7-Dibromomethyl-anthraquinone (5.838 g, 14.8 mmol) and PPh_3 (27.000 g, 102.9 mmol) were added to a three-neck flask containing *N*,*N*-dimethylformamide (320 mL), then the solution was heated to 100 °C and stirred overnight. The reaction mixture was cooled to room temperature, and toluene (400 mL) was added. The precipitate was filtered and dried under vacuum to give a white solid (10.000 g, 80% yield). m.p. >300 °C. ^{1}H NMR 300 MHz ($CDCl_3$,) δ (ppm) 8.01 (m, 24H), 7.72 (m, 12H), 6.07 (d, J = 15.0 Hz, 4H).

*2.3.3. 2,7-Bis-[2-(4-dimethylamino-phenyl)-vinyl]-anthraquinone (**1**)*

2,7-Bis-[(triphenylphosphonium bromide)]-methyl)-anthraquinone (1.005 g, 1.1 mmol) and 4-dimethylamino-benzaldehyde (0.382 g, 2.6 mmol) were added to a two-neck flask containing absolute *N*,*N*-dimethylformamide (44 mL) under N_2 protection, then NaH (0.113 g, 4.7 mmol) was added into the solution. The solution was heated to 100 °C and stirred for 20 h. Water (150 mL) was added slowly after the solution was cooled to room temperature. The formed precipitate was filtered, washed with ethanol (10 mL × 2), and purified by column chromatography on silica gel using a chloroform/petroleum (V/V = 10:1) as eluent. Purple solid (0.250 g, 46% yield) was obtained. m.p >300 °C. IR (KBr, cm^{-1}): 2898, 1683, 1584, 1523, 1359. ^{1}H NMR 300 MHz ($CDCl_3$,) δ (ppm) 8.38 (s, 2H); 8.27 (d, J = 7.8 Hz, 2H); 7.84 (d, J = 7.8 Hz, 2H); 7.50 (d, J = 8.3 Hz, 4H); 7.32 (d, J = 16.3 Hz, 2H); 7.05 (d, J = 16.3 Hz, 2H); 6.75 (d, J = 8.3 Hz, 4H); 3.03 (s, 12H); HRMS. Calcd. for $C_{34}H_{30}N_2O_2$: 498.23073; Found: 498.22912.

*2.3.4. 2,7-Bis-[2-(4-methoxy-phenyl)-vinyl]-anthraquinone (**2**)*

The same procedure as described for **1** gave an orange solid (68% yield). m.p. 245–247 °C. IR (KBr, cm^{-1}): 2929, 1668, 1589, 1509, 1324, 1029. ^{1}H NMR 300 MHz ($CDCl_3$,) δ (ppm) 8.40 (s, 2H); 8.29 (d, J = 8.1 Hz, 2H); 7.87 (d, J = 8.1 Hz, 2H); 7.55 (d, J = 8.3 Hz, 4H); 7.38 (d, J = 16.2Hz, 2H); 7.12 (d, J = 16.2 Hz, 2H); 6.96 (d, J = 8.3 Hz, 4H); 3.86 (s, 6H); HRMS. Calcd for $C_{32}H_{24}O_4$ 472.16746; Found: 472.16784.

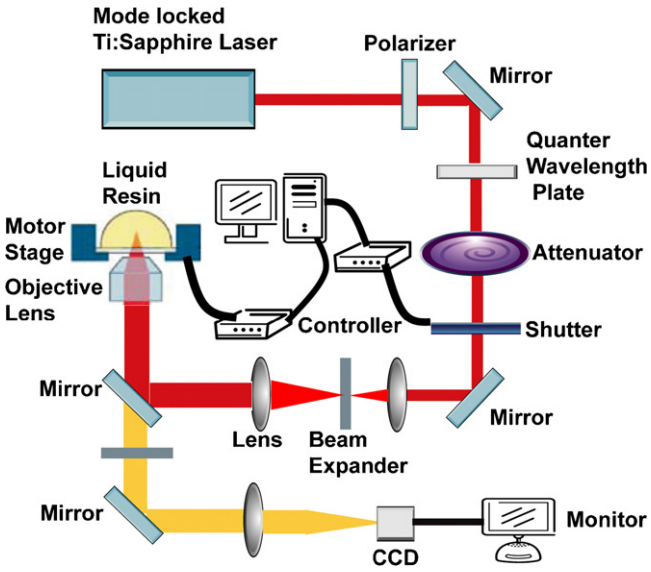

Fig. 1. Experimental setup for two-photon induced polymerization.

2.4. Resin preparation, TPIP and scanning electron microscope (SEM) measurement

Resin was made by mixing MAA (609 mg, 47.43 wt%) as monomer, DEP-6A (673 mg, 52.41 wt%) as crosslinker, **1** or **2** (0.2 mg, 0.02 wt%) as initiator and 1 mL chloroform to improve the solubility of initiator in the resin. After the solvent evaporate, the resin film was transparent. $\boldsymbol{R_1}$ and $\boldsymbol{R_2}$ stand for the resin with compounds **1** and **2**, respectively. The experimental setup for TPIP is shown in Fig. 1. A laser beam from a mode-locked Ti:Sapphire laser system (Tsunami, Spectra-Physics) with a center wavelength of 800 nm, a pulse width of 80 fs, and a repetition rate of 80 MHz was used for all TPIP experiments here. The beam was tightly focused into the resin on a glass cover slip with an oil-immersion objective lens (60×, numerical aperture = 1.42). The resin was scanned by the focused beam in two dimensions (*x*–*y*) with a computer-controlled motor stage. The average laser power was less than 17 mW and the linear scan speeds were 10, 30 and 50 μm/s, respectively. The final structure was obtained after washing out the unpolymerized resin by ethanol. Images of the fabricated lines were observed using a field-emission scanning electron microscope (FE-SEM, JSM-6330F, JOEL). The working voltage and current were 5 kV and 8 μA, respectively.

3. Results and discussion

3.1. Linear optical properties

The UV–vis absorption and fluorescence spectra of **1** and **2** are shown in Fig. 2. All of photophysical data for **1** and **2** are listed in Table 1. These absorption peaks of **1** at 495 nm and **2** at 424 nm correspond to electronic transition from the ground state to the intramolecular charge transfer (ICT) state. The absorption peaks of **1** at 391 nm and **2** at 358 nm are assigned to the typical π–π* transition, locally excited state [28,29]. The absorption

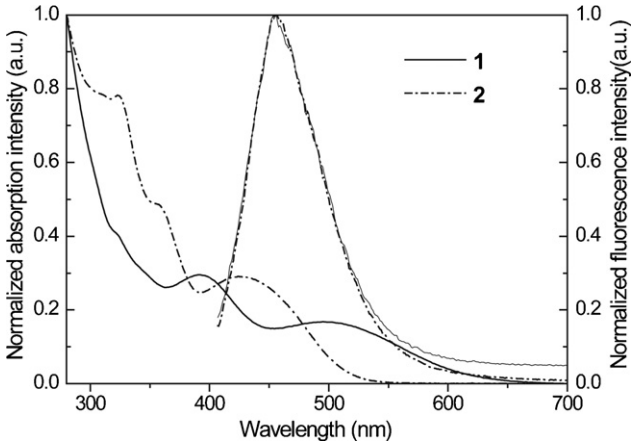

Fig. 2. Normalized UV–vis and fluorescence spectra of **1** and **2**. Solid line denotes UV-absorption and fluorescence of **1**; Dash dot line denotes UV-absorption and fluorescence of **2**.

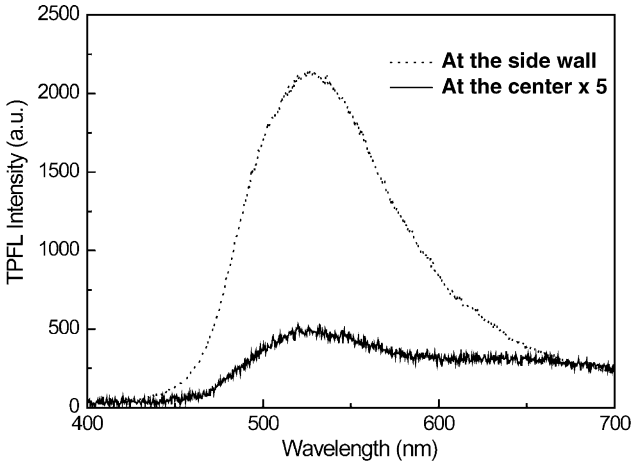

Fig. 3. Two-photon induced fluorescence of **2** at the excitation wavelength of 800 nm. Dot line denotes the focus of light is close to the corner of sample cell; Solid line denotes the focus of light is at the center of sample cell.

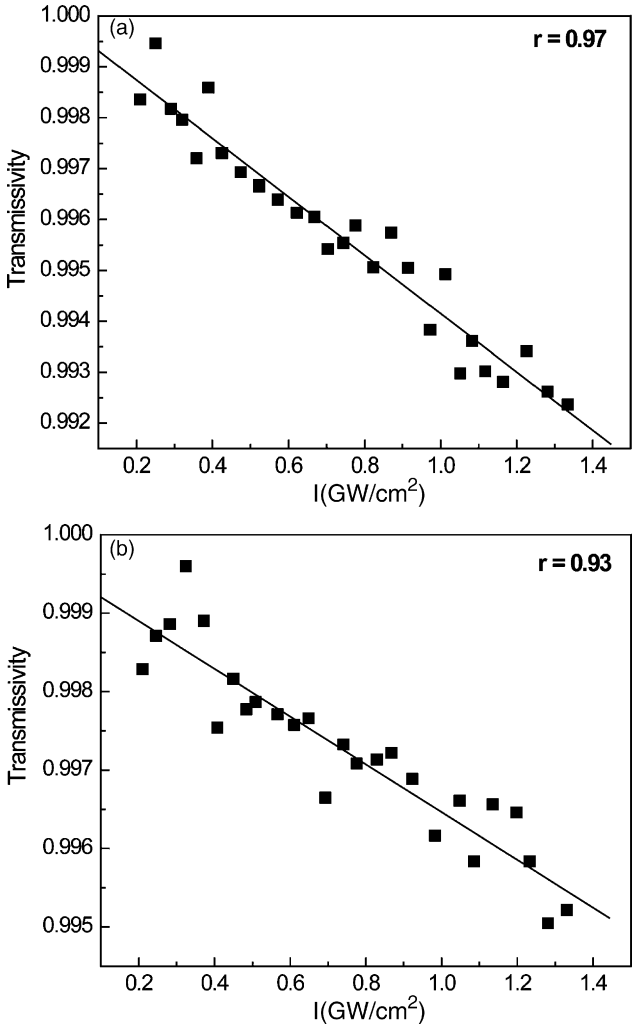

Fig. 4. The plot of transmissivity dependence on light intensity for **1** (a) and **2** (b). Squares denote the experimental value of transmissivity; solid lines denote the theoretical fitting line.

peaks of **1** are red shift comparing with those of **2** due to the stronger electron-donating ability of a dimethylamino group than a methoxy group. The one-photon fluorescence (OPFL) spectra of both compounds were obtained with the excitation wavelength of 400 nm as shown in Fig. 2, in order to compare with the two-photon fluorescence (TPFL) spectra measured at the wavelength of 800 nm for two-photon induced excitation. None of these two spectra has multiple peaks, which indicates that the fluorescence emission occurs from the locally excited state; the ICT singlet state mainly deactivates through a non-radiative decay to ICT triplet state via intersystem crossing. The peaks of OPFL of **1** and **2** localize at the same wavelength

Table 1
One- and two-photon photophysical data of **1** and **2**

Compounds	λ_{max}[a] (nm)	ε[b] (M^{-1} cm^{-1})	λ_{max}^{OPFL}[c] (nm)	Φ_d[d]	λ_{max}^{TPFL}[e] (nm)	β[f] (cm/GW)	$\delta_{800\,nm}$[g] (GM)
1	391	18,000	456	0.018	–	0.012	1635
	495	10,000					
2	358	34,000	456	0.043	526	0.007	995
	424	20,000					

[a] Peak wavelength of one-photon absorption.
[b] Molar extinction coefficient.
[c] Peak wavelength of one-photon fluorescence.
[d] One-photon excited fluorescence quantum yield.
[e] Peak wavelength of two-photon fluorescence.
[f] Nonlinear absorption coefficient due to TPA.
[g] Two-photon absorption cross-section at 800 nm. 1 GM = 10^{-50} cm^4 s $photon^{-1}$.

of 456 nm, which indicates energy differences between locally excited state and ground state for **1** and **2** are the same. The fluorescence quantum yields of **1** and **2** in DMF were determined, according to the fluorescence spectra as shown in Fig. 2, as 0.018 and 0.043, respectively. The low fluorescence quantum yields can be explained to be due to (a) the self-absorption; (b) certain nonradiative decay mechanisms that may arise as a result of "twisted intramolecular charge geometry" acquired by **1** and **2** as a result of electron transfer from the donor group to the acceptor group [30,31]. Lower fluorescence quantum yield of **1** than that of **2** is attributed to charge-transfer bimolecular quenching by the amine [32].

3.2. Non-linear optical properties

Although the TPFL spectra of **1** was failed to be detected due to the present of severe self-absorption at the wavelength region of the TPFL of **1**, the TPFL spectra of **2** was successfully detected since the TPFL of **2** has smaller overlap with the absorption. As shown in Fig. 3, it is clear that the TPFL intensity increases sharply at the excited position close to the corner of sample cell comparing with the excited position at the center. The maximum wavelength of TPFL spectra (λ_{max}^{TPFL}) was localized at 526 nm, which shows red-shift of 70 nm compared to that of one-photon excited fluorescence (λ_{max}^{OPFL}) obtained at the excited wavelength of 400 nm. The results indicated that different excited states occurred between one- and two-photon excitation processes, which might lead to different relaxing processes and emission bands [33].

Nonlinear transmission measurement technique was used to evaluate their δ_{TPA} at the wavelength of 800 nm since two-photon induced fluorescence method is not suitable for the δ_{TPA} measurement of **1** and **2** due to the intense self-absorption and low fluorescence quantum yield [34]. The relationships of transmissivity and light intensity for **1** and **2** are shown in Fig. 4a and b, respectively. It can be seen that the experimental values of **1** and **2** show excellent agreement with their theoretical fitting. Here, the nonlinear absorption coefficient β is obtained from Eq. (1).

$$T_i = \frac{\ln(1 + I_0 L\beta)}{I_0 L\beta} \quad (1)$$

where T_i is transmissivity, I_0 input light intensity, and L is the thickness of the sample solution. T_i can be

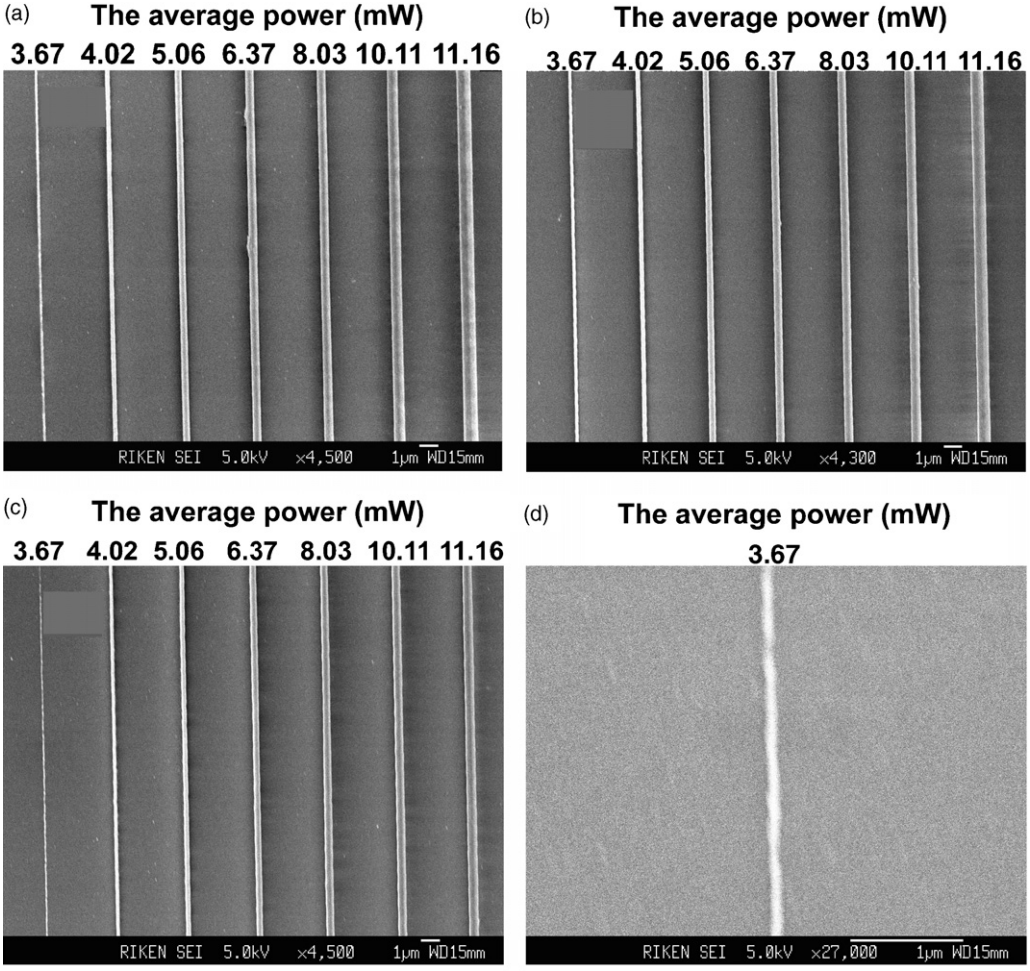

Fig. 5. SEM images of lines fabricated with $\boldsymbol{R_1}$. The linear scan speed of (a), (b), (c) and (d) are 10, 30, 50 and 50 μm/s, respectively. The average power was shown on the above of each line.

obtained from Eq. (2).

$$T_i = \frac{I_i}{I_0} \tag{2}$$

where I_i is light intensity after passing through the sample cell. Therefore, the δ_{TPA} of sample was calculated by Eq. (3).

$$\delta_{TPA} = \left(\frac{h\upsilon\beta}{N_A}\right) \times d \times 10^{-3} \tag{3}$$

where N_A is the Avogadro constant, d the concentration of sample, h plank constant and ν is the wavelength number.

The data for two-photon properties of **1** and **2** obtained by nonlinear transmission method are listed in Table 1. The β values of **1** and **2** were 0.012 and 0.007 cm/GW, respectively. The δ_{TPA} of **1** and **2** were 1635 and 995 GM at 800 nm, respectively. The δ_{TPA} of **1** is much larger than that of **2**, which is due to the stronger intramolecular charge transfer when dimethylamino group is used as a donor comparing with methoxy group. The result shows that the C_{2v} symmetrical anthraquinone derivatives possess large δ_{TPA} as well as low fluorescence quantum yield, which might make them become promising candidates as photoinitiators for TPIP.

3.3. Two-photon induced polymerization

The threshold energy of TPIP and the width of the solid line cured by TPIP were studied for the evaluation of initiating properties on initiators **1** and **2**. The threshold of TPIP presents the lowest laser energy, which can generate enough radicals converting monomers into remaining polymer after development. Here, the polymerization threshold is defined as the lowest average power before being focused by the objective lens, below which the fabricated polymer line cannot form using a linear scan speed of 10 μm/s. The thresholds of $\boldsymbol{R_1}$ and $\boldsymbol{R_2}$ were determined as 3.67 and 8.03 mW, respectively.

The width of cured solid line formed by TPIP, which is the key factor for judging the fabrication resolution, will be mainly influenced by two factors: laser intensity and exposure time. Laser intensity directly determines the region TPA occurred, which defines the volume of radical generation. Exposure time should influence the amount of radicals induced by TPA. The widths of cured solid lines were measured according to the SEM images as shown in Fig. 5. Here, the solid lines were cured by using different average powers with different linear scan speed of 10, 30 and 50 μm/s, in order to investigate the efficiency of initiating polymerization. The relationships between line width and the average power for $\boldsymbol{R_1}$ and $\boldsymbol{R_2}$ are shown in Fig. 6a and b, respectively. For $\boldsymbol{R_1}$ in which initiator **1** was used at the level of 0.02 wt%, the width of lines was decreased from 225 to 185 and 105 nm at the threshold energy of 3.67 mW, when the linear scan speeds increased from 10 to 30 and 50 μm/s, respectively. It was shown that the width of fabricated lines reduced with the increasing of linear scan speed due to decreasing of exposure time when the same average power was used. However, for $\boldsymbol{R_2}$ which included initiator **2** at the same level with $\boldsymbol{R_1}$ of initiator **1**, the line width was 495 nm at the threshold energy of 8.03 mW. Even the linear scan speed was increased to 50 μm/s, the line width was decreased only to 420 nm. It clearly shows that the higher threshold is disadvantageous for obtaining high fabrication resolution in TPIP.

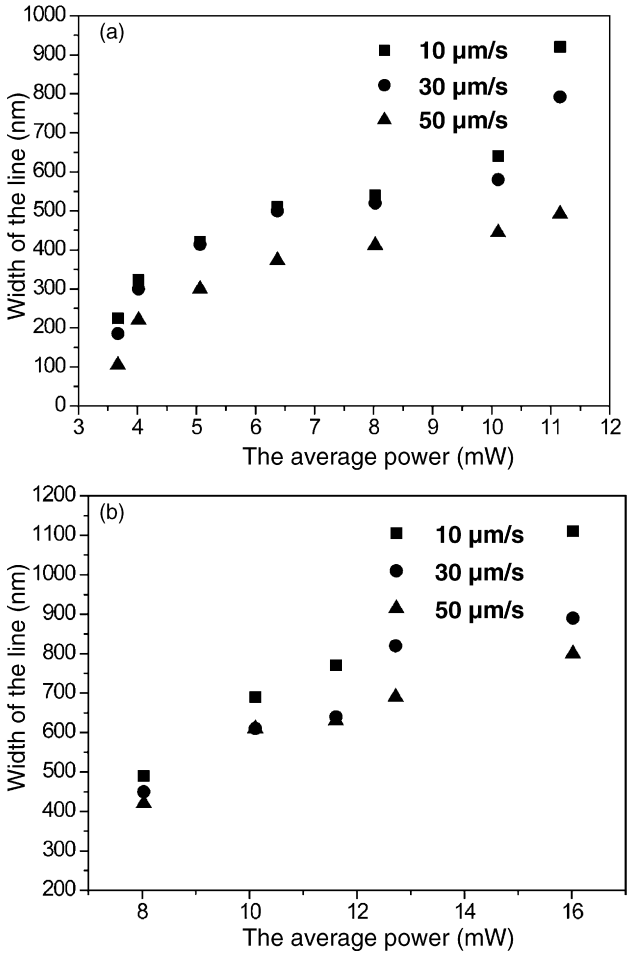

Fig. 6. Width of the Line dependence on the average power for $\boldsymbol{R_1}$ (a) and $\boldsymbol{R_2}$ (b), respectively.

The fact of the lower threshold of $\boldsymbol{R_1}$ than that of $\boldsymbol{R_2}$ indicates that initiator **1** could generate enough radicals to initiate polymerization due to its large δ_{TPA} and higher possibility of nonradiative relaxing process of two-photon induced excited state. The results of narrowing width for cured solid line provide direct evidences to show that the initiator with high initiating efficiency can improve the fabrication resolution of TPIP. These results and discussions here provide a clear direction for the development of TPIP initiator toward improving resolution in microfabrication, which has been excepting for applications in the fields of microdevices and Micro-electromechanical Systems.

4. Conclusion

C_{2v} symmetrical anthraquinone derivatives, 2,7-bis-[2-(4-dimethylamino-phenyl)-vinyl]-anthraquinone and 2,7-bis-[2-(4-methoxy-phenyl)-vinyl]-anthraquinone have been successfully synthesized. Their photophysical properties were evaluated including UV–vis absorption, OPFL and TPFL

as well as TPA. These compounds show large two-photon absorption cross-section at 800 nm and low fluorescence quantum yield. 2,7-Bis-[2-(4-dimethylamino-phenyl)-vinyl]-anthraquinone possesses higher sensitivity compared to 2,7-bis-[2-(4-methoxy-phenyl)-vinyl]-anthraquinone. Investigation on the relationship of resolution and sensitivity indicated higher sensitivity benefits to the improvement of microfabrication resolution.

Acknowledgements

We acknowledge financial support from "One Hundred Oversea Talent" program of Chinese Academy of Sciences (CAS) and CREST and PRESTO program, Japan Science and Technology Agency (JST).

References

[1] T. Kogej, D. Beljonne, F. Meyers, J.W. Perry, S.R. Marder, J.-L. Brédas, Chem. Phys. Lett. 298 (1998) 1.
[2] D. Beljonne, W. Wenseleers, E. Zojer, Z. Shuai, H. Vogel, S.J.K. Pond, J.W. Perry, S.R. Marder, J.-L. Brédas, Adv. Funct. Mater. 12 (2002) 631.
[3] S. Wu, J. Serbin, M. Gu, J. Photochem. Photobiol. A Chem. 181 (2006) 1.
[4] S. Kawata, H.-B. Sun, T. Tanaka, K. Takada, Nature 412 (2001) 697.
[5] S.M. Kuebler, K.L. Braun, W. Zhou, J.K. Cammack, T. Yu, C.K. Ober, S.R. Marder, J.W. Perry, J. Photochem. Photobiol. A Chem. 158 (2003) 163.
[6] G.S. He, J. Swiatkiewicz, Y. Jiang, P.N. Prasad, B.A. Reinhardt, L.-S. Tan, R. Kannan, J. Phys. Chem. A. 104 (2000) 4805.
[7] B.A. Reinhardt, L.L. Brott, S.J. Clarson, A.G. Dillard, J.C. Bhatt, R. Kannan, L. Yuan, G.S. He, P.N. Prasad, Chem. Mater. 10 (1998) 1863.
[8] S.J.K. Pond, M. Rumi, M.D. Levin, T.C. Parker, D. Beljonne, M.W. Day, J.-L. Brédas, S.R. Marder, J.W. Perry, J. Phys. Chem. A. 106 (2002) 11470.
[9] W.-H. Lee, H. Lee, J.-A. Kim, J.-H. Choi, M. Cho, S.-J. Jeon, B.R. Cho, J. Am. Chem. Soc. 123 (2001) 10658.
[10] D.W. Brousmiche, J.M. Serin, J.M.J. Fréchet, G.S. He, T.-C. Lin, S.-J. Chung, P.N. Prasad, R. Kannan, L.-S. Tan, J. Phys. Chem. B. 108 (2004) 8592.
[11] M. Albota, D. Beljonne, J.-L. Brédas, J.E. Ehrlich, J.-Y. Fu, A.A. Heikal, S.E. Hess, T. Kogej, M.D. Levin, S.R. Marder, D. McCord-Maughon, J.W. Perry, H. Röckel, M. Rumi, G. Subramaniam, W.W. Webb, X.-L. Wu, C. Xu, Science 281 (1998) 1653.
[12] B.H. Cumpston, S.P. Ananthavel, S. Barlow, D.L. Dyer, J.E. Ehrlich, L.L. Erskine, A.A. Heikal, S.M. Kuebler, I.-Y.S. Lee, D. McCord-Maughon, J. Qin, H. Röckel, M. Rumi, X.-L. Wu, S.R. Marder, J.W. Perry, Nature 398 (1999) 51.
[13] C. Martineau, G. Lemercier, C. Andraud, I. Wang, M. Bouriau, P.L. Baldeck, Synth. Met. 138 (2003) 353.
[14] Y.-X. Yan, X.-T. Tao, Y.-H. Sun, W.-T. Yu, C.-K. Wang, G.-B. Xu, J.-X. Yang, X. Zhao, M.-H. Jiang, J. Mater. Sci. 40 (2005) 597.
[15] Y. Ren, X.-Q. Yu, D.-J. Zhang, D. Wang, M.-L. Zhang, G.-B. Xu, X. Zhao, Y.-P. Tian, Z.-S. Shao, M.-H. Jiang, J. Mater. Chem. 12 (2002) 3431.
[16] Y.-X. Yan, X.-T. Tao, Y.-H. Sun, G.-B. Xu, C.-K. Wang, J.-X. Yang, X. Zhao, M.-H. Jiang, J. Solid. State. Chem. 177 (2004) 3007.
[17] S.C.N. Montoya, L.R. Comini, M. Sarmiento, C. Becerra, I. Albesa, G.A. Argüello, J.L. Cabrera, J. Photochem, Photobiol A: Biol. 78 (2005) 77.
[18] P. Brodard, A. Sarbach, J.-C. Gumy, T. Bally, E. Vauthey, J. Phys. Chem. A. 105 (2001) 6594.
[19] G.K. Pullen, N.S. Allen, M. Edge, I. Weddell, R. Swart, F. Catalina, S. Navaratnam, Eur. Polym. J. 32 (1996) 943.
[20] N.S. Allen, G. pullen, M. Shah, M. Edge, L. Weddell, R. Swart, F. Catalina, Polymer 36 (1995) 4665.
[21] W.J. Yang, D.Y. Kim, M.-Y. Jeong, H.M. Kim, Y.K. Lee, X. Fang, S.-J. Jeon, B.R. Cho, Chem. Eur. J. 11 (2005) 4191.
[22] M. Nag, W.S. Jenks, J. Org. Chem. 69 (2004) 8177.
[23] T.Y. Ohulchanskyy, D.J. Donnelly, M.R. Detty, P.N. Prasad, J. Phys. Chem. B. 108 (2004) 8668.
[24] M.N. Berberan-Santos, J.M.M. Garcia, J. Am. Chem. Soc. 118 (1996) 9391.
[25] G.T. Morgan, E.A. Coulson, J. Chem. Soc. (1929) 2551–2559.
[26] G. Jones II, W.R. Jackson, C.-Y. Choi, W.R. Bergmark, J. Phys. Chem. 89 (1985) 294.
[27] G.S. He, G.C. Xu, P.N. Prasad, B.A. Reinhardt, J.C. Bhatt, A.G. Dillard, Opt. Lett. 20 (1995) 435.
[28] D. Beljonne, J.-L. Brédas, M. Cha, W.E. Torruellas, G.I. Stegeman, J.W. Hofstraat, W.H.G. Horsthuis, G.R. Möhlmann, J. Chem. Phys. 103 (1995) 7834.
[29] Z.R. Grabowski, K. Rotkiewicz, W. Rettig, Chem. Rev. 103 (2003) 3899.
[30] M. Lal, L. Levy, K.S. Kim, G.S. He, X. Wang, Y.H. Min, S. Pakatchi, P.N. Prasad, Chem. Mater. 12 (2000) 2632.
[31] Q. Song, C.E. Evans, P.W. Bohn, J. Phys. Chem. 97 (1993) 13736.
[32] J. Yang, A. Dass, A.-M.M. Rawashdeh, C. Sotiriou-Leventis, M.J. Panzner, D.S. Tyson, J.D. Kinder, N. Leventis, Chem. Mater. 16 (2004) 3457.
[33] K.D. Belfeld, K.J. Schafer, Y. Liu, J. Liu, X. Ren, E.W. Van Stryland, J. Phys. Org. Chem. 13 (2000) 837.
[34] C. Xu, W.W. Webb, J. Opt. Soc. Am. B. 13 (1996) 481.